

# Structure and Activity of a New Low-Molecular-Weight Heparin Produced by Enzymatic Ultrafiltration

LI FU,<sup>1,2</sup> FUMING ZHANG,<sup>3</sup> GUOYUN LI,<sup>2,4</sup> AKIHIRO ONISHI,<sup>2</sup> UJJWAL BHASKAR,<sup>3</sup> PEILONG SUN,<sup>1</sup> ROBERT J. LINHARDT<sup>2,3,5,6</sup>

<sup>1</sup>Department of Biotechnology, College of Biological and Environmental Engineering, Zhejiang University of Technology, Hangzhou 310032, China

<sup>2</sup>Department of Chemistry and Chemical, Center for Biotechnology and Interdisciplinary Studies, Rensselaer Polytechnic Institute, Troy, New York 12180

<sup>3</sup>Department of Chemical and Biological Engineering, Biology, Troy, New York 12180

<sup>4</sup>College of Food Science and Technology, Ocean University of China, Qingdao, Shandong 266003, China

<sup>5</sup>Department of Biology, Center for Biotechnology and Interdisciplinary Studies, Rensselaer Polytechnic Institute, Troy, New York 12180

<sup>6</sup>Department of Biomedical Engineering, Center for Biotechnology and Interdisciplinary Studies, Rensselaer Polytechnic Institute, Troy, New York 12180

Received 25 January 2014; revised 21 February 2014; accepted 21 February 2014

Published online 14 March 2014 in Wiley Online Library (wileyonlinelibrary.com). DOI 10.1002/jps.23939

**ABSTRACT:** The standard process for preparing the low-molecular-weight heparin (LMWH) tinzaparin, through the partial enzymatic depolymerization of heparin, results in a reduced yield because of the formation of a high content of undesired disaccharides and tetrasaccharides. An enzymatic ultrafiltration reactor for LMWH preparation was developed to overcome this problem. The behavior, of the heparin oligosaccharides and polysaccharides using various membranes and conditions, was investigated to optimize this reactor. A novel product, LMWH-II, was produced from the controlled depolymerization of heparin using heparin lyase II in this optimized ultrafiltration reactor. Enzymatic ultrafiltration provides easy control and high yields (>80%) of LMWH-II. The molecular weight properties of LMWH-II were similar to other commercial LMWHs. The structure of LMWH-II closely matched heparin's core structural features. Most of the common process artifacts, present in many commercial LMWHs, were eliminated as demonstrated by 1D and 2D nuclear magnetic resonance spectroscopy. The antithrombin III and platelet factor-4 binding affinity of LMWH-II were comparable to commercial LMWHs, as was its *in vitro* anticoagulant activity. © 2014 Wiley Periodicals, Inc. and the American Pharmacists Association *J Pharm Sci* 103:1375–1383, 2014

**Keywords:** low molecular weight heparin; heparin lyase; ultrafiltration; anticoagulant; NMR; mass spectrometry; surface plasmon resonance; polymeric drugs; structure-activity relationship; enzymes

## INTRODUCTION

Heparin [also known as unfractionated heparin (UFH)] is a polysaccharide-based anticoagulant drug that was first introduced into clinical practice nearly 100 years ago.<sup>1</sup> Low-molecular-weight heparins (LMWHs), derived from UFH, were more recently introduced, nearly 35 years ago.<sup>1,2</sup> The need for heparin and LMWHs continues to increase as modern medical treatments and procedures, such as the treatment of deep vein thrombosis, postsurgical control of clots,<sup>3,4</sup> extracorporeal therapy (i.e., kidney dialysis and heart–lung oxygenators), and the use of indwelling heparinized catheters and shunts, expand in first-world countries and are introduced in third-world countries.

The major repeating disaccharide unit of heparin is  $\alpha$ -L-IdoA2S(1→4)- $\alpha$ -D-GlcNS6S (where IdoA is idopyranosyluronic acid, S is sulfo, and GlcN is 2-deoxy, 2-amino glucopyranose), but the minor disaccharide units are also present with different structural and sulfation patterns that are integral to heparin's major therapeutic activity, the inhibition of coagulation cascade proteases, thrombin (factor IIa) and factor Xa.

A well-studied pentasaccharide sequence in heparin having the structure,  $\rightarrow$ 4)- $\alpha$ -D-GlcNAc6S(1→4)- $\beta$ -D-GlcA(1→4)- $\alpha$ -D-GlcNS3S6S(1→4)- $\alpha$ -L-Ido2S(1→4)- $\alpha$ -D-GlcNS6S(1→ (where GlcA is glucopyranosyluronic acid and Ac is acetyl) is critical to heparin's specific activation of the serine protease inhibitor antithrombin III (ATIII). Heparin is able to bind both ATIII and thrombin to afford a ternary complex, inactivating thrombin and thus preventing fibrin clot formation. FXa does not interact directly with heparin but is instead inhibited by heparin–ATIII binary complex. The inactivation of thrombin by ATIII requires the longer heparin chains (>15 saccharide units) common to UFH, whereas small heparin chains (from 5 to 15 saccharide units) common to LMWH are capable of binding only ATIII, inactivating factor Xa. Thus, LMWHs are considered factor Xa-selective anticoagulant/antithrombotic drugs.<sup>1,5</sup>

The major physiologic role of platelet factor-4 (PF4), which is released from the alpha-granules of activated platelets, is to bind and neutralize heparin and heparan sulfate on the endothelial surface of blood vessels, thereby inhibiting local ATIII activation and promoting coagulation. The heparin–PF4 complex is the antigen in heparin-induced thrombocytopenia (HIT), an idiosyncratic autoimmune reaction to the administration of the anticoagulant heparin. LMWHs have a lower binding affinity for PF4 than does heparin, which both improve their anticoagulant activity and reduce their incidence of HIT.<sup>6,7</sup> Finally,

Correspondence to: Robert J. Linhardt (Telephone: +518-276-3404; Fax: +518-276-3405; E-mail: linhar@rpi.edu)

*Journal of Pharmaceutical Sciences*, Vol. 103, 1375–1383 (2014)

© 2014 Wiley Periodicals, Inc. and the American Pharmacists Association

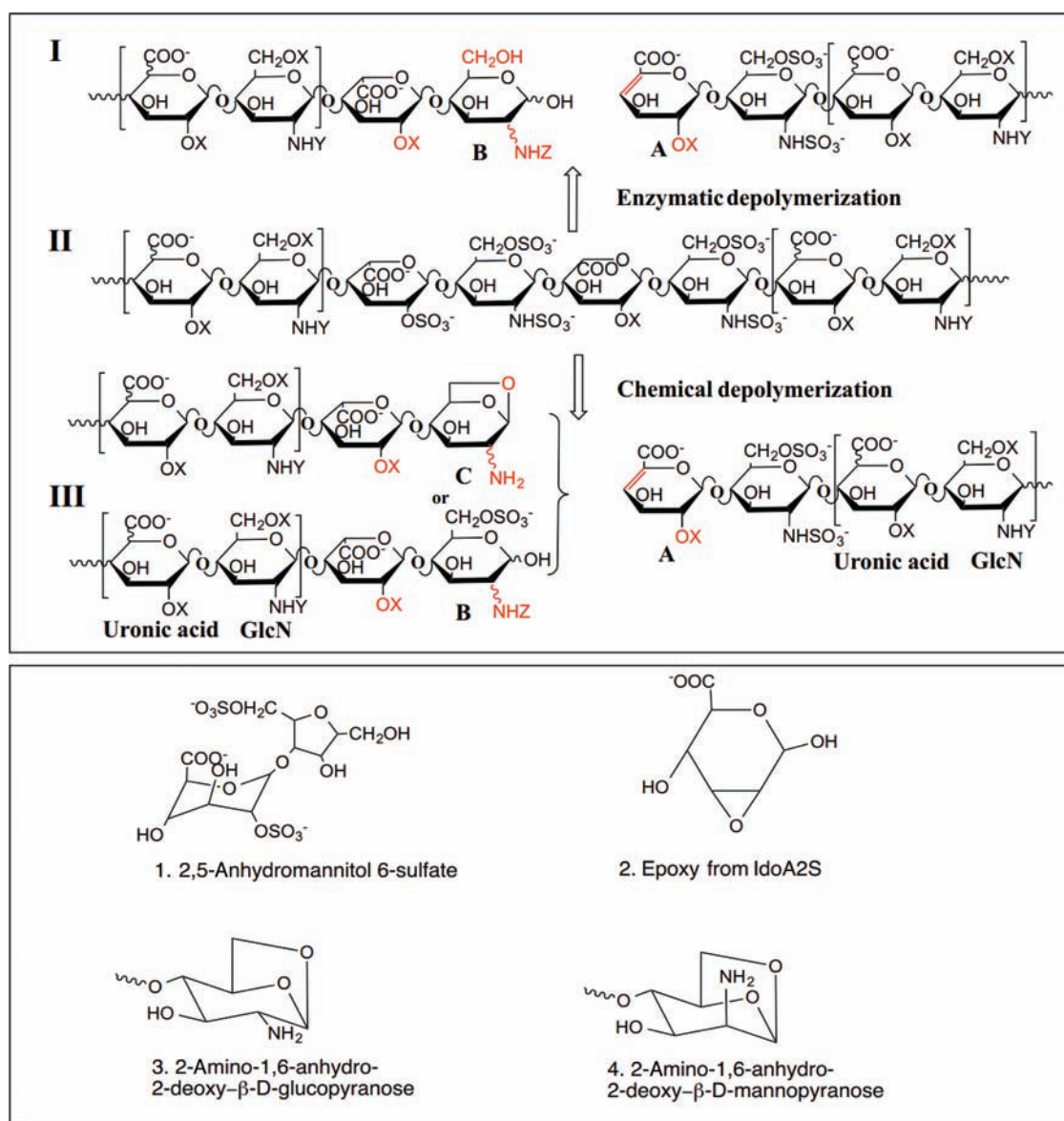


**Figure 1.** Structural features and process artifacts in LMWHs. Upper panel: Major structures of a LMWH prepared using heparin lyase I, Tinzaparin (I), UFH from porcine intestine (II), and commercial LMWH, Enoxaparin (III). (X = SO<sub>3</sub><sup>-</sup> or H; Y = SO<sub>3</sub><sup>-</sup> or Ac<sup>-</sup>; Z = SO<sub>3</sub><sup>-</sup>, Ac<sup>-</sup> or H). Lower panel: Process artifacts present in LMWHs prepared using chemical processes.

the enhanced subcutaneous bioavailability and improved pharmacodynamics of LMWHs have increased the clinical use of these anticoagulants in recent years.<sup>1,8</sup>

Currently, the commercial preparation of LMWHs from UFH includes the controlled chemical depolymerization of heparin by peroxidative cleavage, nitrous acid cleavage, and chemical β-elimination (Fig. 1, upper panel, II–III). These chemical methods result in process artifacts including 2,6-anhydromannitol (Fig. 1, lower panel, structure 1), epoxide (Fig. 1, lower panel, structure 2), 1,6-anhydroglucopyranose (Fig. 1, lower panel, structure 3), and 1,6-anhydromannopyranose (Fig. 1, lower panel, structure 4), as a result of harsh reaction conditions that are used in their preparation.<sup>9,10</sup> In contrast, enzymatic depolymerization, a much milder approach, has also been used to make LMWH. Heparin lyase I, isolated from *Flavobacterium heparinum*, is most commonly used to enzymatically

depolymerize heparin (Fig. 1, upper panel, II to I).<sup>8,11–13</sup> Previous studies, however, demonstrate that although both heparin lyase I and II can cleave →4)-α-D-GlcNS6S(1→4)-α-L-IdoA2S(1→ linkage, heparin lyase I is highly selective for →4)-α-D-GlcNS3S6S(1→4)-α-L-IdoA2S(1→ and heparin lyase II has selectivity for →4)-α-D-GlcNS6S(1→4)-α-L-IdoA(1→.<sup>14,15</sup>

Heparin lyases can be used under mild conditions (room temperature at physiologic pH) to afford LMWHs (Fig. 1, panel I) with fewer process artifacts generated through side reactions. However, enzymatic depolymerization without chain length control can easily result in the overdigestion of heparin, converting an active LMWH into smaller chains without bioactivity, such as disaccharides and tetrasaccharides. Moreover, the heparin lyases, particularly heparin lyase I, are known to selectively act at linkages present within the ATIII–pentasaccharide binding site<sup>15</sup> making the loss of anticoagulant activity

particularly hard to control. Thus, the efficient separation of bioactive oligosaccharides throughout the reaction, protecting them from full depolymerization, is crucial to obtain active LMWH in high yield. In this report, we developed an enzymatic ultrafiltration reactor for LMWH preparation employing mild heparin lyase-catalyzed depolymerization conditions with simultaneous product separation. The chemical structure and *in vitro* bioactivity of the resulting LMWH products were characterized.

## MATERIALS AND METHODS

### Materials

Unfractionated porcine heparin sodium salt 200 U/mg was from Celsus (Cincinnati, Ohio) and bovine heparin sodium salt 150 U/mg was from Sigma Chemical Company (St. Louis, Missouri). Recombinant *Flavobacterium heparinum* heparin lyase I, II and III were expressed in our laboratory using *Escherichia coli* strains, provided by Professor Jian Liu (University of North Carolina, College of Pharmacy, Chapel Hill, North Carolina).<sup>16</sup> Heparin oligosaccharides, from hexasaccharide to icosasaccharide, were used as calibrants for molecular weight determination by size-exclusion chromatography (SEC) and were purchased from Iduron (Manchester, UK). Unsaturated heparan sulfate–heparin disaccharide standards (0S,  $\Delta$ UA-GlcNAc; NS,  $\Delta$ UA-GlcNS; 6S,  $\Delta$ UA-GlcNAc6S; 2S,  $\Delta$ UA2S-GlcNAc; 2SNS,  $\Delta$ UA2S-GlcNS; NS6S,  $\Delta$ UA-GlcNS6S; 2S6S,  $\Delta$ UA2SGlcNAc6S; and TriS,  $\Delta$ UA2S-GlcNS6S, where  $\Delta$ UA is deoxy- $\alpha$ -L-threo-hex-4-enopyranosyl uronic acid) were obtained from Seikagaku Corporation (Chuo-ku, Tokyo, Japan). ATIII and PF4 were from Aniara (West Chester, Ohio).

### Ultrafiltration Behavior of Heparin Oligosaccharides in Various Membranes

Ultrafiltration behavior of heparin oligosaccharides was tested using four different molecular weight cutoff (MWCO) membranes, 3, 5, 10, and 30 kDa. Bovine lung heparin partially digested with heparin lyase I<sup>17</sup> (10 mg in 1 mL distilled water) was filtered through (10,000g at 22°C) an Amicon centrifugal filter with a 30-kDa MWCO membrane (Millipore, Billerica, Massachusetts). The retained fraction was collected (30KT) and the permeate fraction was next filtered through 10-kDa MWCO membrane; the retained (10KT) and permeate fractions were again collected. In the same way, 5KT and 3KT fractions were collected using 5- and 3-kDa membranes, respectively. The final permeate fraction (3KP) obtained using a 3-kDa MWCO membrane was also collected.

Defined heparin-derived oligosaccharides,<sup>18</sup> each of a different degree of polymerization (dp)8 (MW ~2653 Da), dp10 (MW ~3317 Da), and dp12 (MW ~3980 Da) (1 mg each), were individually filtered through 3-, 5-, and 10-kDa MWCO membranes. All of the retained and permeate fractions of dp8, dp10, and dp12 were collected and lyophilized for carbazole assay<sup>19</sup> and polyacrylamide gel electrophoresis (PAGE) analysis.<sup>17</sup>

### Enzymatic Ultrafiltration Reactor

The enzymatic ultrafiltration reactor setup consisted of a 50-mL stirred ultrafiltration cell unit (Model 8050; Millipore) connected with a pressure-controllable nitrogen cylinder and a magnetic stirrer. Unfractionated porcine heparin (100 mg) was dissolved in 25 mL of reaction buffer

[40 mM ammonium acetate and 3 mM calcium acetate (pH 7.0)]. The reaction was initiated by adding heparin lyase I or heparin lyase II into the ultrafiltration reactor equipped with 10-KDa membrane (Millipore) under 2 or 20 psi N<sub>2</sub> pressure (as controlled by a nitrogen cylinder regulator) at room temperature (22°C). When the reaction volume was reduced to 5 mL, the pressure was released and the reactor was refilled by adding 15 mL of reaction buffer before resuming filtration at the same pressure. The permeate fraction was monitored using ultraviolet spectrophotometry at 232 nm. All of the permeate fractions were pooled, concentrated, and desalted by dialysis with 3-kDa MWCO membrane. The final desalted product (LWMH) was lyophilized for further quantification and for structure/activity analysis. Different amounts of heparin lyase I or II, and different operating pressures were tested to optimize product yields.

### SEC of Heparin for Molecular Weight Measurement

Size-exclusion chromatography was performed using TSK-GEL G3000PWxI size-exclusion column (Tosoh Corporation, Minato-Ku, Tokyo, Japan) with a sample injection volume of 20  $\mu$ L and a flow rate of 0.6 mL/min on an apparatus composed of a Shimadzu LC-10Ai pump, a Shimadzu CBM-20A controller, and a Shimadzu RID-10A refractive index detector (Shimadzu, Kyoto, Japan). The mobile phase consisted of 0.1 M aqueous NaNO<sub>3</sub>. The column was maintained at 40°C during the chromatography with an Eppendorf column heater (Eppendorf, Hamburg, Germany). The SEC chromatograms were recorded with the LC solution version 1.25 software (Shimadzu, Kyoto, Japan) and analyzed with its “GPC Postrun” function. The molecular weight determination was carried out as previously reported.<sup>20</sup>

### Polyacrylamide Electrophoresis

Heparin oligosaccharide samples were analyzed by PAGE using 0.75 mm  $\times$  6.8 cm  $\times$  8.6 cm minigels cast from 22% resolving gel monomer solution and 5% stacking gel monomer solution, and LMWHs and UFH were analyzed by PAGE using 0.75 mm  $\times$  6.8 cm  $\times$  8.6 cm minigels cast from 15% resolving gel monomer solution and 5% stacking gel monomer solution. Each sample of 10  $\mu$ g was loaded into the gel; purified dp10 and partially digested bovine lung heparin<sup>17</sup> were used as molecular markers. The minigels were subjected to electrophoresis at a constant 200 V for 110 min and visualized with 0.5% (w/v) alcian blue in 2% (v/v) aqueous acetic acid solution.<sup>17</sup>

### Nuclear Magnetic Resonance Analysis

Low-molecular-weight heparin samples were analyzed by <sup>1</sup>H, <sup>13</sup>C nuclear magnetic resonance (NMR), and two-dimensional NMR spectroscopy. Heteronuclear single-quantum coherence (HSQC), proton–proton correlation spectroscopy (HHCOSY) and total correlation spectroscopy (TOCSY) were used to characterize their structures.<sup>2,21</sup> All NMR experiments were performed on Bruker Advance II 600 MHz spectrometer (Bruker Bio Spin, Billerica, Massachusetts) with Topsis 2.1.6 software (Bruker Bio Spin). Samples were dissolved in 0.5 mL <sup>2</sup>H<sub>2</sub>O (99.996%; Sigma Chemical Company) and freeze-dried repeatedly to remove the exchangeable protons. The samples were redissolved in 0.4-mL <sup>2</sup>H<sub>2</sub>O and transferred to NMR microtubes (outside diameter; 5 mm; Norell, Landisville, New Jersey). The conditions for one-dimensional <sup>1</sup>H NMR spectra were as follows: wobble sweep width of 12.3 kHz, acquisition time of

2.66 s, and relaxation delay of 8.00 s. Temperature was 298 K. The conditions for two-dimensional HSQC spectra were as follows: 32 scans, sweep width of 6.15 kHz, acquisition time of 0.33 s, and relaxation delay of 0.90 s. The conditions for two-dimensional HHCOSY spectra were as follows: 16 scans, sweep width of 7.46 kHz, acquisition time of 0.28 s, and relaxation delay of 1.50 s.<sup>20</sup>

### Enzymatic Digestion for Disaccharide Analysis and Tetrasaccharide Mapping

For disaccharides analysis, the heparin lyase I, II, and III (10 mU each) in 5  $\mu$ L of 25 mM Tris (hydroxymethyl) amino methane (Tris), 500 mM NaCl, 300 mM imidazole buffer (pH 7.4) were added to 10  $\mu$ g LMWH sample in 25  $\mu$ L of distilled water and incubated at 35°C for 10 h to completely degrade the heparin sample. The products were recovered by centrifugal filtration using an YM-10 microconcentrator (Millipore), and the heparin disaccharides were recovered in permeate and freeze-dried. The resulting heparin disaccharides were dissolved in water to concentration of 50–100 ng/2  $\mu$ L for liquid chromatography (LC)–mass spectrometric (MS) analysis.<sup>8,22</sup> For tetrasaccharides analysis, the heparin lyase II [40 mU in 20  $\mu$ L of 25 mM Tris, 500 mM NaCl, 300 mM imidazole buffer (pH 7.4)] was added to 50–100  $\mu$ g heparin sample in 40  $\mu$ L of distilled water and incubated at 35°C for 10 h. The degraded production was freeze-dried for subsequent LC–MS analysis.<sup>8</sup>

### Disaccharide Analysis and Tetrasaccharide Mapping Using LC–MS

Liquid chromatography–mass spectrometry analyses were performed on an Agilent 1200 LC/MSD instrument (Agilent Technologies, Inc., Wilmington, Delaware) equipped with a 6300 ion trap and a binary pump followed by a UV detector equipped with a high-pressure cell.<sup>23</sup> The column used was a Poroshell 120 C18 column (2.1  $\times$  100 mm<sup>2</sup>; 2.7  $\mu$ m; Agilent Technologies, Inc.). Eluent A was water/acetonitrile (85:15, v/v), and eluent B was water/acetonitrile (35:65, v/v). Both eluents contained 12 mM TrBA and 38 mM ammonium acetate with pH adjusted to 6.5 with acetic acid. For disaccharides analysis, a gradient of solution A for 5 min followed by a linear gradient from 5 to 15 min (0%–40% solution B) was used at flow rate of 150  $\mu$ L/min.

For tetrasaccharide analysis,<sup>8</sup> a gradient of solution A for 2 min followed by a linear gradient from 2 to 40 min (0%–30% solution B) was used at a flow rate of 150  $\mu$ L/min. The column effluent entered the source of the electrospray ionization–MS for continuous detection by MS. The electrospray interface was set in the negative ionization mode with a skimmer potential of –40.0 V, a capillary exit of –40.0 V, and a source temperature of 350°C, to obtain the maximum abundance of the ions in a full-scan spectrum (200–1500 Da). Nitrogen (8 L/min, 40 psi) was used as a drying and nebulizing gas.

### Surface Plasmon Resonance Analysis

Biotinylated heparin prepared from Celsus heparin was immobilized to sensor chip SA (streptavidin) (GE Healthcare, Uppsala, Sweden) based on the manufacturer's protocol. Surface plasmon resonance (SPR) measurements were performed on a BIAcore 3000 (GE Healthcare) operated using the version software. Solution competition studies between surface heparin and soluble different LMWHs to measure IC<sub>50</sub> were performed using SPR.<sup>5</sup> ATIII (250 nM) mixed with different of

concentrations (0, 9.4, 18.8, 37.5, 75, 150, 300  $\mu$ g/mL) of heparin and PF4 (125 nM) mixed with different of concentrations (0, 3.2, 6.3, 12.5, and 25.0  $\mu$ g/mL) of heparin in HBS-EP buffer {10 mM of 2-[4-(2-hydroxyethyl)piperazin-1-yl]ethanesulfonic acid, 150 mM sodium chloride, 3 mM ethylenediaminetetraacetic acid (EDTA), 0.005% polysorbate surfactant P20, pH 7.4}(GE Healthcare) were injected over heparin chip at a flow rate of 30  $\mu$ L/min, respectively. After each run, the chip was regenerated with 1 min injections each of glycine pH 2.5 and 2 M NaCl. For each set of competition experiments on SPR, a control experiment (only protein without heparin) was performed to make sure the surface was completely regenerated and that the results obtained between runs were comparable.

### Anti-FIIa and Anti-FXa Assays

The anti-Xa and anti-IIa activities of LMWHs were determined using BIOPHEN Heparin Anti-Xa (two stage) and Anti-IIa (two stage) kits (Aniara, West Chester, Ohio). Human ATIII 40 mU in 80  $\mu$ L R1 buffer (Tris 0.05 M, NaCl 0.175 M, EDTA 0.0075 M, at pH 8.40 containing polyethylene glycol at 0.1%, and sodium azide as preservative) was used for anti-Xa assay. Human ATIII 10 mU in 80  $\mu$ L R2 buffer (Tris 0.05 M, NaCl 0.175 M, EDTA 0.0075 M, at pH 8.40 containing bovine serum albumin at 0.2%, and sodium azide as preservative) mixed with different masses of heparin (range from 0, 5, 10, 15, and 20 ng) were incubated for 2 min at 37°C. Then, purified bovine factor Xa (320 ng in 40  $\mu$ L R1 buffer) or purified human thrombin (960 mU in 40  $\mu$ L in R2 buffer) preincubated at 37°C were added and incubated for 2 min before the addition of chromogenic substrate specific for factor Xa [CS-01(65), 1.2 mM, 40  $\mu$ L] or the chromogenic substrate specific for thrombin [CS-01(38), 1.25 mM, 40  $\mu$ L]. The reaction mixture was incubated at 37°C for 2 min for anti-Xa assay and 1 min for anti-IIa assay and then stopped with citric acid (20 mg/mL, 80  $\mu$ L). The absorbance was measured at 405 nm. Anti-Xa and anti-IIa activities were calculated using a standard curve of different concentrations of heparin (0–1 U/mL).

## RESULTS AND DISCUSSION

### Behavior of Heparin Oligosaccharides in Membrane Filtration

Most commercial ultrafiltration membranes with controlled MWCO are calibrated based on spherically shaped analytes, such as globular proteins. Pore size is a critical parameter for the development of the ultrafiltration reactor. Therefore, the behavior of linear, rod-like heparin oligosaccharides was investigated using commercial membranes having various pore sizes. PAGE analysis clearly demonstrated that oligosaccharides smaller than dp10 (MW ~2687 Da) were nearly absent in 30KT and 10KT fractions (Fig. 2b). Moreover, oligosaccharides prominent in these fractions were relatively long heparin chains of molecular weight of more than 5500 Da. In contrast, the 5KT and 3KT fractions contained oligosaccharides of shorter chain lengths having molecular weights between 1000 and 6400 Da. Disaccharides (dp2, MW ~663 Da) and tetrasaccharides (dp4, MW ~1326 Da) were the major oligosaccharides found in the 3KP fraction. The ultrafiltration experiments on purified dp8, dp10, and dp12 oligosaccharides using 3-, 5-, and 10-kDa MWCO membrane provided the recovery yields of these oligosaccharides as a function of membrane pore size (Table 1). The recovery was reduced as the molecular size of

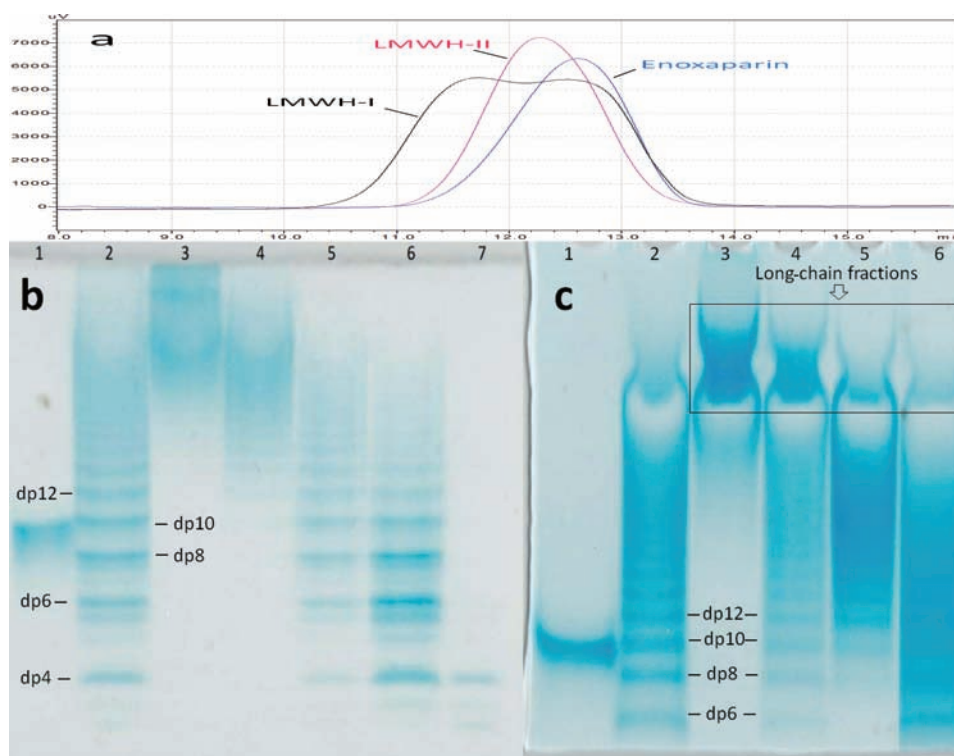


**Figure 2.** Molecular weight analysis of LMWHs. (a) SEC analysis of LMWHs; (b) PAGE analysis of heparin oligomers trapped on the different MWCO membranes: Lane 1, dp10; lane 2, partially digested bovine lung heparin ladder; lane 3, 30KT; lane 4, 10KT; lane 5, 5KT; lane 6, 3KT; lane 7, 3KP. (c) PAGE analysis of LMWHs: lane 1, dp10; lane 2, partially digested bovine lung heparin ladder; lane 3, UFH; lane 4, LMWH-I; lane 5, LMWH-II; lane 6, Enoxaparin.

**Table 1.** Permeation Ratio of Purified Heparin Oligomers by Membranes

Membrane Pore Size	Oligosaccharide Permeation Percentages (%)		
	dp8	dp10	dp12
3-KDa	15.6	6.4	3.5
5-KDa	29.5	23.3	7.6
10-KDa	61.7	53.4	47.4

oligosaccharide became larger for each membrane tested and the recovery yield of the oligosaccharides tested all increased as the membrane pore size increased. On the basis of the molecular weight of the expected for a typical LMWH product (3000–8000 Da), a 10-kDa membrane was selected for optimal product recovery by enzymatic ultrafiltration.

### Heparin Enzymatic Ultrafiltration

Six different enzymatic ultrafiltration reactions were examined, two of which afforded LMWH-I and LMWH-II (Table 2). Relatively high pressure (20 psi) and a 10-kDa membrane afforded the best product recoveries of over 80% (determined by carbazole assay,<sup>19</sup> based on a linear standard curve  $y = 0.0184x + 0.1132$ ,  $r^2 = 0.99$ ) with reactions of 2 h at room temperature. These results suggest that enzymatic ultrafiltration offers a scalable alternative for the preparation of LMWH. The molecular weight data obtained on UFH, commercial LMWHs, LMWH-I, and LMWH-II showed that LMWH-I and LMWH-II had molecular weight properties comparable with commercial LMWHs (Table 3). However, LMWH-I showed higher poly-

**Table 2.** Different Reactions and Products of Enzymatic Ultrafiltration

Reaction	Products	Enzyme	N <sub>2</sub> Pressure (psi)	Yield (%)
R1		Heparin lyase I, 120 mU	2	30.5
R2		Heparin lyase I, 250 mU	2	38.2
R3	LMWH-I	Heparin lyase I, 250 mU	20	80.1
R4		Heparin lyase II, 120 mU	2	20.8
R5		Heparin lyase II, 250 mU	2	35.7
R6	LMWH-II	Heparin lyase II, 250 mU	20	81.6

dispersity as a result of a large portion of long-chain product (Table 3, Figs. 2a and 2c). In contrast, LMWH-II was comparable to commercial LMWHs on the basis of both average molecular weight and polydispersity and contained fewer long-chain fractions (Table 3, Figs. 2a and 2c). Thus, based on the molecular weight analyses, our focus turned to LMWH-II for further characterization.

### NMR Analysis

1D <sup>1</sup>H NMR and 2D HHCOSY, TOCSY and HSQC NMR were carried out to characterize the structure of LMWH-II. The 1D <sup>1</sup>H NMR spectra of Enoxaparin and UFH looked quite similar,

**Table 3.** Average Molecular Weight of Heparins Using SEC

Sample	$M_N$	$M_w$	$M_w/M_N$
UFH	14618 ± 114	24899 ± 244	1.7
LMWH-I	5500 ± 30	8560 ± 80	1.6
LMWH-II	5090 ± 50	6250 ± 60	1.2
Enoxaparin	3190 ± 20	4215 ± 30	1.3
Enoxaparin <sup>a</sup>	4372 ± 231	5629 ± 233	1.3
Dalteparin <sup>a</sup>	5835 ± 271	6626 ± 222	1.1
Tinzaparin <sup>a</sup>	5833 ± 223	7333 ± 155	1.2

<sup>a</sup>Data based on the results from Achour et al.<sup>26</sup>

except the  $\Delta$ UA unit (peak a, Fig. 3a) formed from the chemical depolymerization. In LMWH-II, calcium-induced chemical shifts of  $I_{2S}$  protons at H1 and H5 were observed in both 1D  $^1$ H NMR (Fig. 3a) and 2D HSQC spectra (Figs. 3b and 3c).<sup>24</sup> This is not surprising as calcium was in the buffer used to prepare LMWH-II. Other peaks of LMWH-II in  $^1$ H NMR spectra looked similar to that of commercial LMWH and UFH. The anomeric signals of the reducing and nonreducing ends in LMWH-II from the cleaved  $\rightarrow 4$ GlcNS6S(1 $\rightarrow$ 4)IdoA2S(1 $\rightarrow$  and  $\rightarrow 4$ )GlcNS6S(1 $\rightarrow$ 4)IdoA(1 $\rightarrow$  linkages (Fig. 1, panel I) were all found in HSQC spectra (Fig. 3b); other internal saccharide signals for LMWH-II could be fully assigned from the HHCOSY, TCOSE, and HSQC spectra (Fig. 4a and 4c). Signals from the side products (process artifacts) of chemical  $\beta$ -eliminative depolymerization in commercial LMWH were hidden behind the

major heparin signals so were invisible in 1D  $^1$ H NMR; however, in 2D HSQC spectra, these process artifacts can be clearly seen. The  $\Delta$ UA<sub>2S</sub> and  $\Delta$ UA<sub>2OH</sub> signals, overlapped HSQC spectra of LMWH-II and in Enoxaparin, the 1,6-anhydro-glucopyranose (cross-peak C1, Figs. 1, lower panel structure 3, and 3b), 1,6-anhydro-mannopyranose (cross-peak C2, Figs. 1, lower panel structure 4, and 3b), and epoxide from alkaline treatment of  $I_{2S}$  (Fig. 1, lower panel structure 2) were found in Enoxaparin. By contrast, none of these process impurities were observed in LMWH-II. The 2,5-anhydromannitol residue (Fig. 1, lower panel structure 1), having the 3.9–4.3 ppm proton and 80–90 ppm carbon cross-peaks,<sup>10</sup> was also not present in LMWH-II.

### Disaccharide Analysis and Tetrasaccharide Mapping

Heparin can be nearly completely converted to disaccharides through its treatment with heparin lyases I, II, and III. Although disaccharide analyses of heparin have been previously published,<sup>21,22</sup> the results of these analyses are dependent on the analytical method used and interlab variation can be high. In the current study, the disaccharide analysis of heparin, LMWH-II, and Enoxaparin were performed back-to-back in triplicate (Table 4). As both LMWH-II and Enoxaparin were prepared from porcine-derived UFH, their disaccharide composition was similar. A notable exception was the level of TriS, which is enriched in LMWH-II and the level of 6S and NS6S, which are diminished in LMWH-II. These subtle changes in disaccharide composition comes from the preferential

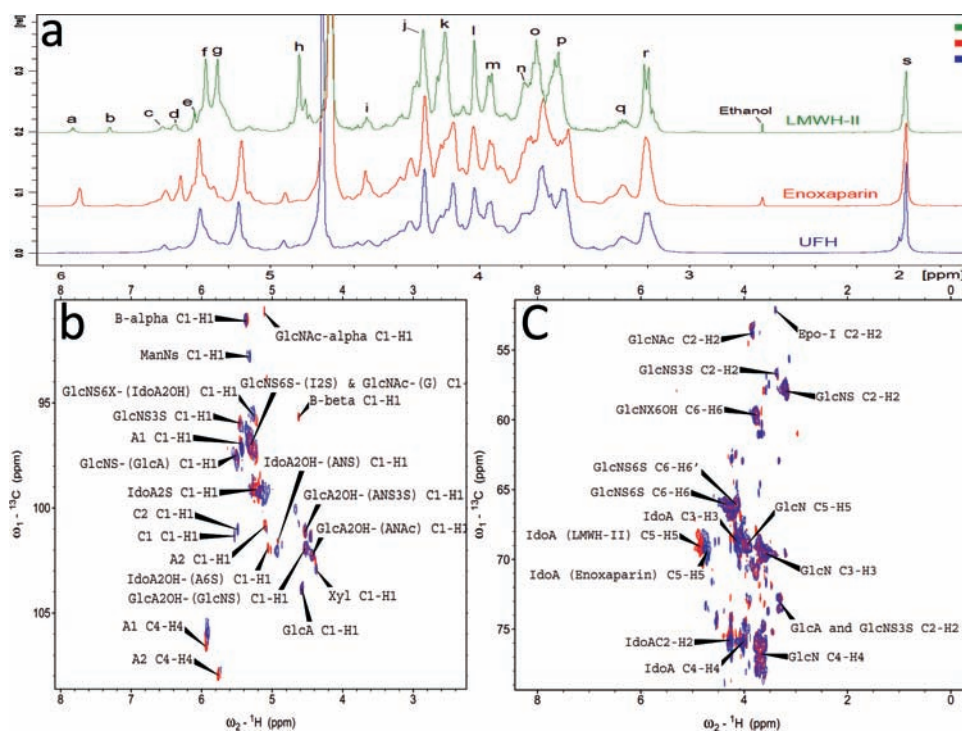


**Figure 3.** 1D  $^1$ H NMR and 2D HSQC spectra of heparins. (a) Comparison and assignments for UFH, Enoxaparin, and LMWH-II. (a) H4  $\Delta$ UA<sub>2S</sub>; (b)  $\Delta$ UA<sub>2OH</sub>; (c) H1  $A_{NS6X-(G)}$ ; (d) H1  $A_{NS3S}$ ; (e) B ( $z = H$ ) molecule of  $\alpha$ -configuration in panel I and III of Figure 1; (f) H1  $A_{NS6X-(I_{2S})}$  and  $A_{NAc6X-(G)}$ ; (g) H1  $I_{2S}$ ; (h) H5  $I_{2S}$ ; (i) H1 G; (j) H2  $I_{2S}$ ; (k) H3  $I_{2S}$ ; (l) H4  $I_{2S}$ ; (m), H5  $A_{NS6S}$ ; (n) H6  $A_{NS}$ ; (o) H4  $A_{NS6S}$ ; (p) H3  $A_{NS6X}$ ; (q) H2 G and  $A_{3S,3SNS}$ ; (r) H2  $A_{NS6X}$ ; (s) acetyl CH3 (A, glucosamine; I, iduronic acid; G, glucuronic acid). (b) Anomeric region comparison and assignments for LMWH-II (red) and enoxaparin (blue). A1 and A2,  $\Delta$ UA<sub>2OH</sub> and  $\Delta$ UA<sub>2OH}, two types of A molecules in panel I and III of Figure 1; B-alpha and B-beta, B ( $z = H$ ) molecules of  $\alpha$  and  $\beta$  configurations in panel I and III of Figure 1; C1 (Fig. 1, panel 3) and C2 (Fig. 1 panel 4), C molecules in Figure 1, panel III. (c) Aliphatic region comparison and assignments for LMWH-II (red) and enoxaparin (blue). Epo-I, epoxide formed from the alkaline treatment of  $I_{2S}$  (Fig. 1, panel 2). Selected signals were labeled based on the assignments of Guerrini et al.<sup>25</sup></sub>

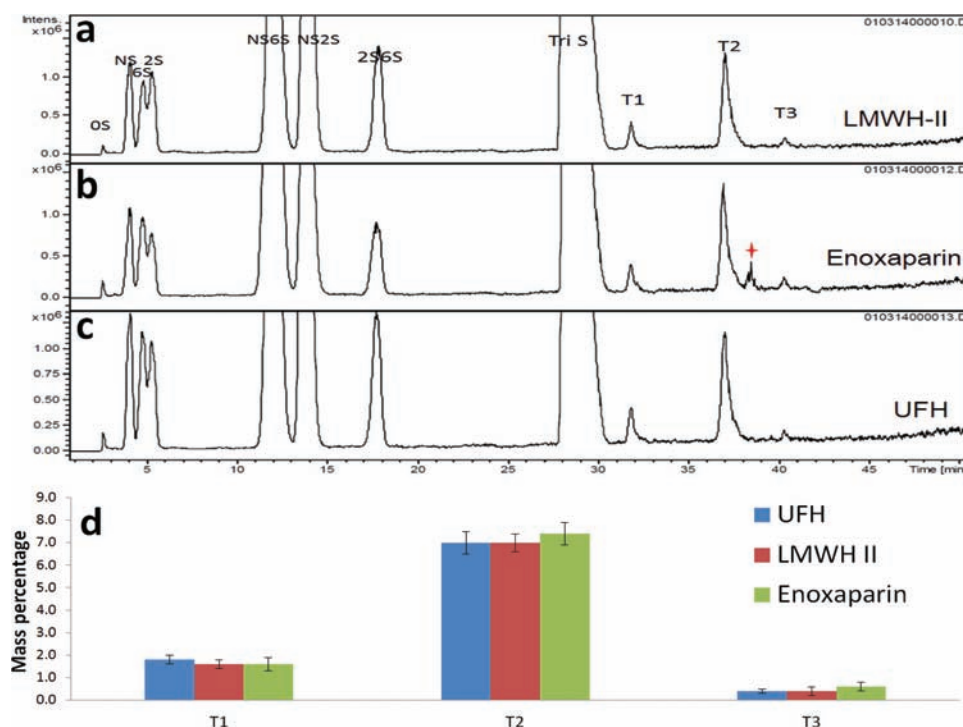


**Figure 4.** Tetrasaccharide mapping data for LMWH-II, Enoxaparin, and UFH. Extracted ion chromatography of LMWH-II (a), Enoxaparin (b), and UFH (c). The star indicates unidentified tetrasaccharide peak. (d) The relative mass percentages of the heparin lyase II-resistant tetrasaccharides. T1,  $\Delta$ UA-GlcNAc6S-GlcA-GlcNS3S; T2,  $\Delta$ UA-GlcNAc6S-GlcA-GlcNS3S6S; T3,  $\Delta$ UA-GlcNS6S-GlcA-GlcNS3S6S.

**Table 4.** Heparin Disaccharide Composition Analysis by LC-MS.

Samples	Heparin disaccharides composition (%)							
	$\Delta$ Di-0S	$\Delta$ Di-NS	$\Delta$ Di-6S	$\Delta$ Di-2S	$\Delta$ Di-NS6S	$\Delta$ Di-NS2S	$\Delta$ Di-2S6S	$\Delta$ Di-TriS
UFH	0.8 $\pm$ 0.2	1.9 $\pm$ 0.1	2.4 $\pm$ 0.5	1.4 $\pm$ 0.5	14.1 $\pm$ 0.8	5.4 $\pm$ 0.2	1.5 $\pm$ 0.2	72.6 $\pm$ 0.3
LMWH-II	0.6 $\pm$ 0.3	1.8 $\pm$ 0.3	<b>1.9 <math>\pm</math> 0.5</b>	1.6 $\pm$ 0.4	<b>10.5 <math>\pm</math> 0.7</b>	5.3 $\pm$ 0.3	1.6 $\pm$ 0.2	<b>76.8 <math>\pm</math> 0.1</b>
Enoxaparin	0.6 $\pm$ 0.5	1.8 $\pm$ 0.5	2.2 $\pm$ 0.8	1.1 $\pm$ 0.4	15.2 $\pm$ 0.9	4.3 $\pm$ 0.4	1.7 $\pm$ 0.3	73.1 $\pm$ 0.2

Data shown in bold indicate significant compositional differences between LMWH-II and UFH and Enoxaparin.

**Table 5.** Composition and Molecular Mass of Tetrasaccharides Formed in Mapping Experiment

Fractions	<i>m/z</i>	Calculated Molecular Mass	Theoretical Molecular Mass	Sequence
T1	[477.4] <sup>2-</sup>	956.8	956.1	$\Delta$ UA-GlcNAc6S-GlcA-GlcNS3S
T2	[517.4] <sup>2-</sup>	1036.8	1036	$\Delta$ UA-GlcNAc6S-GlcA-GlcNS3S6S
T3	[536.3] <sup>2-</sup>	1074.6	1074	$\Delta$ UA-GlcNS6S-GlcA-GlcNS3S6S

cleavage of heparin lyase II at sites containing these disaccharide sequences resulting in their presence in disaccharides and tetrasaccharide products eliminated by enzymatic ultrafiltration.

When heparin or LMWH is exhaustively treated with heparin lyase I, II, and III in addition to the formation of disaccharides, some lyase-resistant tetrasaccharides are also formed (Figs. 4a-4c) because of the presence of 3-*O*-sulfo containing glucosamine residues.<sup>22</sup> There are three major types of these heparin lyase II-resistant tetrasaccharides (T1–T3) as previously shown (Table 5).<sup>20</sup> Their molecular ratio provides a fingerprint of the heparin from which they are derived as well as an insight into the structural diversity of the AT-binding pentasaccharide sequence within heparin. Using tetrasaccharide standards,<sup>22</sup> a standard curve was constructed to calculate the relative dis-

tribution of these sites. As LMWH-II and Enoxaparin are both derived from UFH prepared from porcine intestinal mucosa, the percentages of three tetrasaccharides were present at the similar levels (Fig. 4d). In commercial LMWH, an unexpected peak appeared between T2 and T3 tetrasaccharides peaks in extracted ion chromatography (Fig. 5b). We believe that this peak is associated with tetrasaccharide side products (process artifacts, see Fig. 1, lower panel) formed under the harsh chemical reaction conditions used to prepare Enoxaparin.

#### SPR Analysis

High ATIII affinity and low PF4-binding affinity are critical for the clinical utility of a LMWH. Previously, we described the application of a competitive SPR-binding assay for heparin.<sup>20</sup>

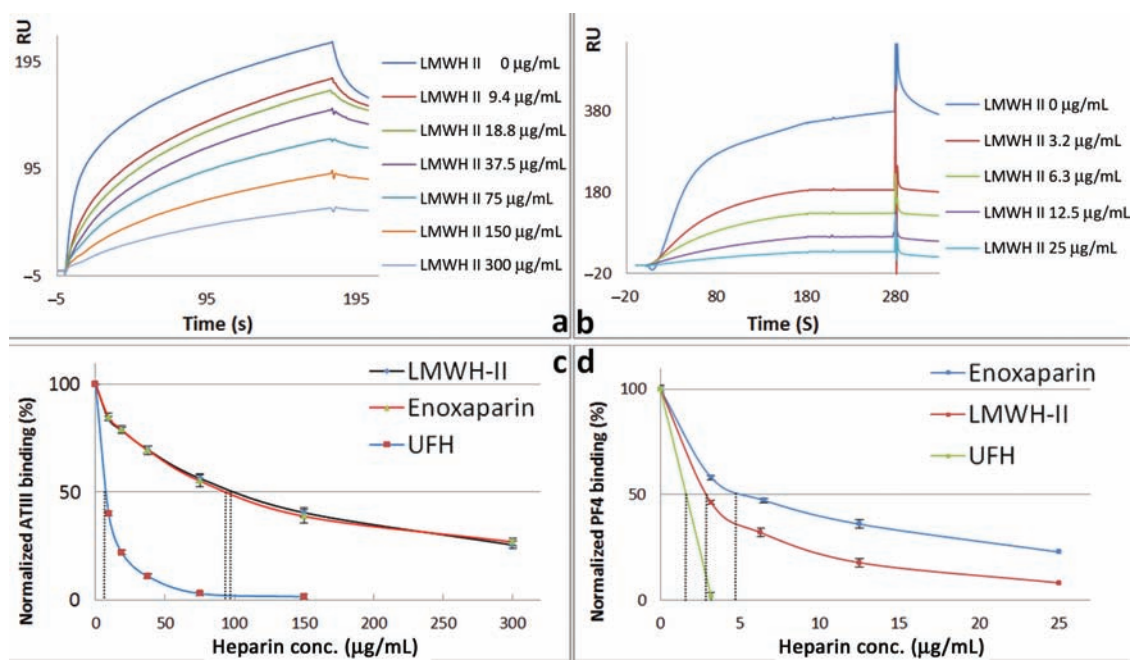


**Figure 5.** Surface plasmon resonance sensorgrams and IC<sub>50</sub> measurement of LMWH-II, Enoxaparin, and UFH using surface competition SPR. (a) Competition SPR sensorgrams of ATIII–heparin interaction (solution LMWH/surface heparin competition); (b) competition SPR sensorgrams of PF4–heparin interaction (solution LMWH/surface heparin competition); (c) IC<sub>50</sub> measurement for ATIII binding; (d) IC<sub>50</sub> measurement for PF4 binding.

Using SPR, solution/surface competition experiments were performed to determine the relative binding affinity of different heparins to ATIII and PF4. ATIII (500 nM) or PF4 (25 nM) were mixed with different concentrations of heparin in HBS-EP buffer were injected over heparin chip. Once the active binding sites on ATIII molecules were occupied by heparin in the solution, the binding of ATIII or PF4 to the surface-immobilized heparin is prevented, resulting in a reduction in SPR signal (Figs. 5a and 5b). The IC<sub>50</sub> values (concentration of competing analyte resulting in a 50% decrease in response units) were calculated from the plots (normalized ATIII or PF4 binding signal vs. heparin concentration in solution). ATIII-binding affinity of heparin is dependent on the presence of an ATIII-binding site structure within a heparin chain.<sup>1</sup> The calculated ATIII IC<sub>50</sub> value of LMWH-II was comparable to Enoxaparin (Fig. 5c). The decrease of ATIII-binding affinity of LMWH-II compared with UFH is probably caused by the loss of a small number of ATIII-binding sites during the enzymatic depolymerization. PF4-binding affinity is dependent on the molecular weight of the heparin product being tested.<sup>26,7</sup> Thus, as expected, LMWH-II showed significantly lower PF4-binding compared with UFH but higher than that of Enoxaparin (Fig. 5d).

#### Anti-Xa and Anti-IIa activities

The anti-Xa and anti-IIa activities of LMWH-II were next measured to investigate the anticoagulant activity properties of LMWH-II produced by enzymatic ultrafiltration (Table 6). As expected, UFH shows identical anti-Xa and anti-IIa activity with an anti-Xa/anti-IIa ratio of 1 (Table 6). The anti-Xa and anti-IIa activities of Enoxaparin were similar to the values reported in other recent publications.<sup>9,24</sup> The anti-Xa/anti-IIa ratio of LMWH-II was 2.74 is within the range of values for other commercial LMWHs (2.38–4.10).<sup>26</sup>

**Table 6.** Anti-Xa and Anti-IIa Activity of UFH, LMWH-II, and commercial LMWHs

Heparin	Anti-Xa Activity (U/mg)	Anti-IIa Activity (U/mg)	Anti-Xa/Anti-IIa (Ratio)
UFH	201	201	1
LMWH-II	163 ± 4	59 ± 6	2.7
Enoxaparin	170 ± 5	47 ± 4	3.6
Enoxaparin <sup>a</sup>	184 ± 2	45 ± 3	4.1
Nadroparin <sup>a</sup>	178 ± 9	67 ± 4	2.7
Dalteparin <sup>a</sup>	172 ± 6	93 ± 9	2.4
Tinzaparin <sup>a</sup>	181 ± 7	45 ± 3	3.9

<sup>a</sup>Data based on the results from Achour et al.<sup>26</sup>

#### CONCLUSIONS

In the current study, enzymatic ultrafiltration is used to obtain an 80% yield of LMWH-II in 2 h at room temperature. This is an improvement over the reported product recoveries in other recent investigations.<sup>26, 28</sup> Economic considerations are critical in the preparation of LMWH, like any other commercial product. Although photochemical preparation of LMWHs can result in up to 93% yields, this approach requires 12 h and is difficult to scale.<sup>9</sup> Mild enzymatic depolymerization may be an ideal approach to produce LMWH because it is scalable, affords high recoveries of product, and avoids the formation of product artifacts that are common in harsh chemical processes. The use of ultrafiltration in an enzymatic process promotes the recovery of primarily active chains providing good process control on product activity. Activity analysis and tetrasaccharide mapping also demonstrate that enzymatic ultrafiltration protects the crucial active ATIII-binding pentasaccharide. Further studies will be required to access the *in vivo* biological

activities and pharmacological efficacy of LMWH-II and to examine process scale-up.

## ACKNOWLEDGMENT

This work was supported by grants from the National Institutes of Health HL101721 and HL096972.

## REFERENCES

- Linhardt RJ. 2003. Heparin: Structure and activity. *J Med Chem* 46:251–254.
- Guerrini M, Zhang Z, Shriver Z, Naggi A, Masuko S, Langer R, Casu B, Linhardt RJ, Torri G, Sasisekharan R. 2009. Orthogonal analytical approaches to detect potential contaminants in heparin. *Proc Natl Acad Sci USA* 106:16956–16961.
- Weintraub AY, Sheiner E. 2007. Anticoagulant therapy and thromboprophylaxis in patients with thrombophilia. *Arch Gynecol Obstet* 276:567–571.
- Bick RL, Frenkel EP, Walenga J, Fareed J, Hoppensteadt DA. 2005. Unfractionated heparin, low molecular weight heparins, and pentasaccharide: Basic mechanism of actions, pharmacology, and clinical use. *Hematol Oncol Clin North Am* 19:1–51.
- Beaudet J, Weyers A, Solakyildirim K, Yang B, Takiuddin M, Mousa S, Zhang F, Linhardt RJ. 2011. Impact of autoclave sterilization on the activity and structure of formulated heparin. *J Pharm Sci* 100:3396–3404.
- Eisman R, Surrey S, Ramachandran B, Schwartz E, Poncz M. 1990. Structural and functional comparison of the genes for human platelet factor 4 and PF4alt. *Blood* 76:336–344.
- Warkentin TE. 2007. Drug-induced immune-mediated thrombocytopenia from purpura to thrombosis. *N Engl J Med* 356:891–893.
- Xiao Z, Tappen BR, Mellisa LY, Zhao W, Canova LP, Guan H, Linhardt RJ. 2011. Heparin mapping using heparin lyase and the generation of a novel low molecular weight heparin. *J Med Chem* 54:603–610.
- Higashi K, Hosoyama S, Ohno A, Masuko S, Yang B, Sterner E, Wang Z, Linhardt RJ, Toida T. 2012. Photochemical preparation of a novel molecular weight heparin. *Carbohydr Polym* 87:1737–1743.
- Keire DA, Buhse LF, Al-Hakim A. 2013. Characterization of currently marketed heparin products: Composition analysis by 2D-NMR. *Anal Methods* 5:2984–2994.
- Yang VC, Linhardt RJ, Bernstein H, Cooney CL, Langer R. 1985. Purification and characterization of heparinase from *Flavobacterium heparinum*. *J Biol Chem* 260:1849–1857.
- Lohse DL, Linhardt RJ. 1992. Purification and characterization of heparin lyases from *Flavobacterium heparinum*. *J Biol Chem* 267:24347–24355.
- Linhardt RJ, Galliher PM, Cooney CL. 1986. Polysaccharide lyases. *Appl Biochem Biotechnol* 12:135–177.
- Toida T, Hileman RE, Smith AE, Vlahova PI, Linhardt RJ. 1996. Enzymatic preparation of heparin oligosaccharides containing antithrombin III binding sites. *J Biol Chem* 271:32040–32047.
- Xiao Z, Zhao W, Yang B, Zhang Z, Guan H, Linhardt RJ. 2011. Heparinase 1 selectivity for the 3,6-di-O-silfo-2-deoxy-2-sulfamido- $\alpha$ -D-glucopyranose (1,4) 2-O-sulfo- $\alpha$ -L-idopyranosyluronic acid (GlcNS3S6S-IdoA2S) linkage. *Glycobiology* 21:13–22.
- Chen J, Jones CL, Liu J. 2007. Using an enzymatic combinatorial approach to identify anticoagulant heparansulfate structures. *Chem Biol* 14:986–993.
- Edens RF, Al-Hakim A, Weiler JM, Rethwisch DG, Fareed J, Linhardt RJ. 1992. Graduate polyacrylamide gel electrophoresis for determination of the molecular weights of heparin derivatives. *J Pharm Sci* 81:823–827.
- Pervin A, Gallo C, Jandik KA, Han X-J, Linhardt RJ. 1995. Preparation and structural characterization of large heparin-derived oligosaccharides. *Glycobiology* 5:83–95.
- Bitter T, Muir HM. 1962. A modified uronic acid carbazole reaction. *Anal Biochem* 4:330–334.
- Fu L, Li G, Yang B, Onishi A, Li L, Sun P, Zhang F, Linhardt RJ. 2013. Structural characterization of pharmaceutical heparins prepared from different animal tissues. *J Pharm Sci* 102:1447–1457.
- Zhang F, Yang B, Ly M, Solakyildirim K, Xiao Z, Wang Z, Beaudet JM, Torelli AY, Dordick JS, Linhardt RJ. 2011. Structural characterization of heparins from different commercial sources. *Anal Bioanal Chem* 401:2793–2803.
- Linhardt RJ, Rice KG, Kim YS, Lohse DL, Wang HM, Loganathan D. 1988. Mapping and quantification of the major oligosaccharide components of heparin. *Biochem J* 254:781–787.
- Zhang Z, Xie J, Liu H, Liu J, Linhardt RJ. 2009. Quantification of heparan sulfate and heparin disaccharides using ion pairing, reverse-phase, micro-flow, high performance liquid chromatography coupled with electrospray ionization trap mass spectrometry. *Anal Chem* 81:4349–4355.
- Mazák K, Beecher CN, Kraszni M, Larive CK. 2014. The interaction of enoxaparin and fondaparinux with calcium. *Carbohydr Res* 384:13–19.
- Guerrini M, Guglieri M, Naggi A, Sasisekharan R, Torri G. 2007. Low molecular weight heparins: Structural differentiation by bidimensional nuclear magnetic resonance spectroscopy. *Semin Thromb Hemost* 33:478–487.
- Achour O, Bridiau N, Godhbani A, Joubioux FL, Juchereau SB, Sannier F, Piot JM, Arnaudin IF, Maugard T. 2013. Ultrasonic-assisted preparation of a low molecular weight heparin (LMWH) with anticoagulant activity. *Carbohydr Polym* 97:1737–1743.
- Wu J, Zhang C, Mei X, Li Y, Xing XH. 2014. Controllable production of low molecular weight heparins by combinations of heparinase I/II/III. *Carbohydr Polym* 101:484–492.
- Mikhailov D, Young HC, Linhardt RJ, Mayo KH. 1999. Heparin decasaccharide binding to platelet factor-4 and growth-related protein-a: Introduction of a partially folded state and implications for heparin induced thrombocytopenia. *J Biol Chem* 274:25317–25329.